Capillary Condensation in Linear Mesopores of Different Shape

D. Wallacher,[1] N. Künzner,[2] D. Kovalev,[2] N. Knorr,[3] and K. Knorr[1]

[1]*Technische Physik, Universität des Saarlandes, D 66041 Saarbrücken, Germany*
[2]*Technische Universität München, Physik-Department E16, D 85747 Garching, Germany*
[3]*Max-Planck-Institut für Polymerforschung, D 55126 Mainz, Germany*

(Received 3 September 2003; published 14 May 2004)

The hysteresis and kinetics of capillary condensation of N_2 and Ar in linear mesopores, produced by etching of Si wafers, have been studied for different pore shapes, including the ink bottle geometry. Pore blocking has been observed in the solid state of the pore fillings, but not in the liquid state. We conclude that individual local geometries such as the pore mouth, a blind end, or a single constriction have no effect on the shape of sorption isotherms, that the pore space should be regarded as a statistical ensemble of pore segments with a lot of quenched disorder.

DOI: 10.1103/PhysRevLett.92.195704 PACS numbers: 64.70.Fx, 05.70.Np, 64.70.Hz, 81.07.–b

Porous composites show a rich variety of effects concerning the propagation of electromagnetic or sound waves, electric transport, or hydraulic mass flow including the displacement of a liquid by another one. The fascinating properties arise from a competition of the intrinsic length scale with the pore size. For pore in the nanometer range, the pore size is usually derived from sorption isotherms [1–3]. Such measurements relate the mass uptake n with the vapor pressure p, are usually performed with N_2 at 77 K, and typically show a reversible section at low p due to the growth of an adsorbed layer on the pore walls followed by the filling of the pores via capillary condensation. Capillary condensation is not only a fine example of a (first order) phase transition, namely, the vapor-liquid transition, in a confined geometry, but is also of relevance for the uptake of moisture in soil, rocks, and masonry and the related effect of frost heave. Capillary condensation shows hysteresis with respect to adsorption and desorption. Condensation occurs at a pressure p_{ads} larger than the pressure p_{des} of evaporation. For routine characterization of pore space, p_{ads} (or p_{des}) is converted into pore size by referring, e.g., to the Kelvin equation. Note, however, that this procedure lacks a sound base. Quite different theoretical models (see below) can be made to fit an experimental isotherm by making suitable assumptions on the pore geometry and the topology of the pore network. This situation is typical for an ''inverse problem.''

The present article reports vapor pressure isotherms of N_2 and Ar in mesoporous Si. Not only are the pores in porous Si of trivial topology, namely, linear and noninterconnected, but also they can be tailored—as we will show—to have different shapes. This will allow us to comment and to question the models and concepts that have been proposed for the hysteresis of capillary condensation.

Starting material is a B-doped Si (100) wafer covered with an epilayer, 18 μm thick. The sample has been electrochemically etched with a current density of 30 mA/cm^2 in a solution of 25% HF, 25% H_2O, and 50% ethanol. These conditions are standard and give noninterconnected pores of polygonal cross section with diameters in the nm range, oriented perpendicular to the surface [4–6]. The pore diameter depends on the doping level and is smaller in the epilayer (D_s) than in the regular part of the wafer (D_l). Four different pore geometries have been produced which are shown schematically in the insets of Fig. 1. Cul-de-sac pores in the epilayer (type A1, diameter D_s), cul-de-sac pores in the regular part of the wafer, obtained by etching the side of the wafer opposite to the epilayer (type A2, D_l). Ink bottle pores (type B) starting with an outer thinner D_s section in the epilayer and a wider D_l section with a blind end in the regular part of the wafer, and finally pores (type C) similar to type B but with a second outlet that has been produced by increasing the etching current so much that the porous double layer was released from the wafer. The samples have been broken into pieces and the broken edges have been inspected by optical and atomic force microscopy. For sample B, three strata, the porous D_s-D_l-double layer and the bulk Si underneath, could be easily identified under the microscopy from the different hue and the thicknesses of the two porous strata have been determined. They are in good agreement to what was inferred from the etching conditions. The AFM images show that the pores are indeed linear with no cross links and oriented along [100]. Volumetric isotherms (Fig. 1) of N_2 at 77.2 K in all four types of pores and of Ar in type B pores at 84.7 and at 63.5 K have been measured using a computer controlled all-metal gas handling system that is equipped with a membrane pressure gauge of 1000 mbar full scale. The capillary condensate is liquid, except for the solid Ar filling of the 63.5 K isotherm. For each data point of an isotherm, the sample has been exposed to the vapor at a pressure slightly different from the pressure of the previous data point and the evolution of p with time t has been recorded until the pressure readings of the last minute were stable within 0.01 mbar, but at least for 5 min.

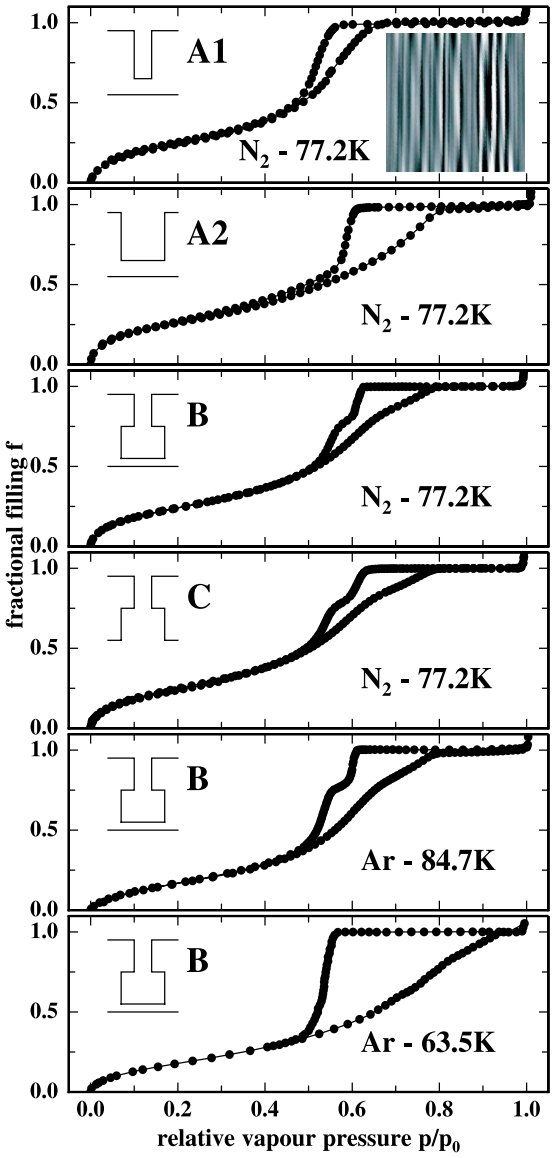

FIG. 1 (color online). Adsorption/desorption isotherms for liquid N_2 at 77.2 K, liquid Ar at 84.7 K and solid Ar at 63.5 K. The different pore geometries, labeled A1, A2, B, and C are included schematically. The inset shows a side view obtained by AFM (95 nm × 95 nm).

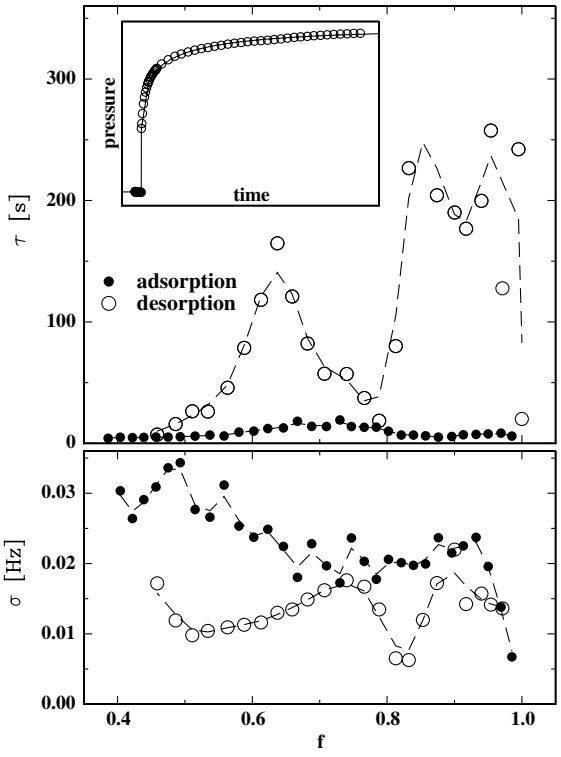

FIG. 2. Upper frame: The pressure relaxation time τ of the stretched exponential decay law as function of the fractional filling f for the 77.2 K isotherm of liquid N_2 in the bottle neck pores of type B. Lower frame: the corresponding mass conductivity. The inset shows the $p(t)$ transient during a desorption step and a fit with a stretched exponential decay.

p was found to approach the new asymptotic value following a stretched exponential decay, $p(t) - p(t = \infty) \sim \exp[-(t/\tau)^{\beta}]$ with β values around 0.5 (Fig. 2). This decay law has been encountered in many "complex" systems and diverse concepts (such as a hierarchical relaxation of constraints) have been proposed for its interpretation [7]. We regard it as an indication of disorder. The relaxation time τ is shown in Fig. 2 as a function of f for the 77 K isotherms of N_2 in pore B.

The pore diameters D_s in the epilayer and D_l in the regular part of the wafer, have been estimated from p_{ads} and/or p_{des} by referring to the Kelvin equation with and without correcting for the thickness of the preadsorbed layer or alternatively to the theory of Ref. [8]. Doing so one assumes that the liquid wets the pore walls completely(that is with vanishing contact angle). This is established for planar Si substrates [9]. The absolute values of D_l and D_s are about 5 to 6 nm. They depend on type of data analysis but the ratio $D_s/D_l = 0.82 \pm 0.02$ does practically not. Altogether these figures are in agreement with the relations of D as function of the doping level and etching conditions shown in Ref. [4].

The isotherms on pores A1 and A2 show the hysteresis loops with a smoothly increasing adsorption branch and a somewhat steeper desorption branch that were encountered in many other studies on mesopores. The desorption branches of the 77 K isotherms of N_2 in type B and C pores show not only one but two steps. (Two analogous features can also be identified in the adsorption branches, though less clearly.) The upper and the lower desorption step occur at pressures that are about identical in type B and C pores and that are close to those observed in pores of type A2 and A1, respectively. Thus the pores B and C consist of two sections with diameters D_s and D_l that fill and empty sequentially. The heights of the two steps are nearly equal showing that the two sections have comparable volumes (as was intended).

The isotherms on liquid Ar ($T = 84.7$ K) and on liquid N_2 ($T = 77.2$ K) in the ink bottle pores of sample B are practically identical. The isotherm on the solid regime of

Ar ($T = 63.5$ K) is clearly different: the substructure of the desorption branch has disappeared, desorption takes place at a pressure that is close to that of the emptying of the D_l section in the liquid regime. Furthermore the adsorption branch is shifted to higher p and consequently is the hysteresis loop much wider than in the liquid regime.

In the following we briefly review theoretical models of capillary condensation, in order to prepare a basis for the discussion thereafter. Capillary condensation is a type of wetting phenomenon and as such it is governed by the ratio and range of the fluid-fluid interaction and the fluid-matrix interaction [10,11]. The theoretical models can be classified according to the degree of disorder they consider. Disorder is brought forth by variations of the pore diameter or of the substrate potential. Models that deal with a single homogeneous pore interpret capillary condensation as a transition taking place at a pressure p_{eq} between a low-density filling at low p to a high-density filling at high p, analogous to the liquid-vapor transition of a bulk van der Waals system (which in fact is recovered for $D \rightarrow \infty$) [8,12–15]. Since the transition involves a qualitative change of the shape of the liquid-vapor interface the transition is of first order with metastable states, vaporlike states with an adsorbed film on the pore walls supersaturated beyond its equilibrium thickness between p_{eq} and p_+, and a stretched metastable liquid between p_{eq} and p_-, $p_- < p_{eq} < p_+$. At p_+ liquid bridges across the pores are formed, at p_- cavitation bubbles nucleate. Whether or not the metastable states can be traced out in an adsorption/desorption cycle depends not only on whether fluctuations can overcome the nucleation barriers but also on the situation at the pore ends. For a pore with open ends, the liquidlike metastable states are irrelevant since the preexisting menisci at the pore mouths can retreat on pore emptying. A blind end eliminates the vaporlike metastable states [6,16] since there is already a meniscus across the pore that can move towards the pore mouth on filling. Thus the liquidlike metastable states are only relevant for closed pores, an unrealistic case, and for blocked pores (see below).

Maximum disorder has been treated theoretically by considering a random matrix [17]. The calculations were based on a site diluted lattice gas model treated in local mean field approximation. They showed that there is a complex free-energy landscape with a large number of metastable configurations that lead to adsorption/desorption hysteresis (even if there is no underlying liquid-vapor transition). The resulting isotherms resemble experimental ones very closely, an observation that suggests that in the experimental system the metastable states just do not have time enough to relax and that accordingly changes of f proceed only when driven by changes of p.

Real porous materials are neither completely random nor do they have homogeneous cylindrical pores. Models try to cover such cases of intermediate disorder by making assumptions on the morphology and the topology of pore space. The pores are assumed to consist of segments of different diameter D, that is of cavities and necks, convergent and divergent sections [2]. The crucial geometry is the ink bottle shape. Thinking of capillary condensation in terms of a phase transition of first order, this geometry leads to pore blocking. In the most rigorous form, the concept of pore blocking assumes that a pore segment with diameter D can only evaporate on lowering the vapor pressure to $p_{eq}(D)$ if there is free access to the vapor reservoir outside the porous matrix; see, e.g., [2]. Thus for pores of type B the evaporation of the segment with the larger diameter D_l is delayed until the segment with the smaller diameter D_s is ready to empty at a pressure $p_{eq}(D_s)$, $p_{eq}(D_s) < p_{eq}(D_l)$. Pore blocking is the basis of percolation models [18–21] which provide an elegant interpretation of the sharp, phase-transition-like onset of desorption in pore networks such as Vycor. Pore blocking can be bypassed by cavitation [22,23], this will happen at $p_-(D_l)$ if $p_-(D_l) > p_{eq}(D_s)$ or by density fluctuations [24](which are the microscopic analogue of cavitation bubbles). For adsorption it is usually assumed that the segments fill independently, every one at the proper value of $p_{eq}(D)$. Alternatively one can argue that this should only be valid if a neighboring segment is already filled [25], such that filling of the D segment can be achieved by the advance of the meniscus but that otherwise filling is delayed to $p_+(D)$.

For the discussion of the present experimental results we borrow arguments from these concepts. The isotherms of cul-de-sac pores in Si (see Ref. [6] and the samples A1 and A2 of Fig. 1) do show hysteresis in contrast to what has been stated above for pores with a blind end. Guided by the calculations on the random matrix we propose that the hysteresis is due to quenched disorder imposed by some variation, δD, of the pore diameter along the pores. δD must be relatively small, smaller than $(D_l - D_s)$, since otherwise one should not have observed two resolved desorption steps for the graded pores B and C. Given the large length-to-diameter ratio of the pores one expects that the pores are chains consisting of a large number of segments with different values of D. It appears plausible that the thermodynamic properties of such a statistical ensemble are not dictated by the presence or absence of a blind end. The idea of quenched disorder to be relevant is also supported by the fact that changes of the filling have been only observed as a consequence of p changes.

The comparison of the results on the four types of samples shows that the D_s and D_l segments of the samples B and C fill and empty sequentially, that it makes no difference whether the D_l segment has to do so via the D_s segment (in sample B) or via its own outlet(s) (in samples A2 and C). Thus the ink bottle type configuration does not lead to pore blocking and it appears that the large number of minor D variations along the segments D_l and D_s is a more effective source for metastable states and hysteresis than the single bottle neck even though the

change of the diameter from D_l to D_s is larger than the variations of D in the two segments.

The 63.5 K isotherm on solid Ar in sample B shows only one desorption step at a pressure p_{des} that is about equal to that of the D_s segment of the liquid state. Thus in the solid state the emptying of the D_l segment is in fact delayed by pore blocking. It would be indeed difficult to imagine how density fluctuations or cavitation could bypass pore blocking in the solid regime. One rather expects that the pores empty by direct sublimation into the vapor reservoir outside such that the solid-vapor interface retreats from the pore mouth. The shift of the adsorption branch to higher p and lower f is presumably related to a change of the wetting behavior from complete wetting in the liquid state to partial wetting in the solid state [11], an important ingredient being the structural mismatch between the amorphous film on the pore walls and the quasibulk crystalline material in the pore center [26]. Thereby the critical thickness of the film at which capillary sublimation occurs is shifted to higher p, thus leading to an increased width of the hysteresis loop.

Figure 2 shows the pressure relaxation time τ of the stretched exponential decay law as function of the filling fraction f for the ink bottle sample B at 77.2 K. τ is maximum during the emptying of the two segments and larger for the D_l than for the D_s segment. In pore C with two outlets the situation is reversed. At first glance this may be taken as an indication for a temporary blocking of the D_l segment in sample B. It turns out, however, that $\tau(f)$ just mimics the f dependence of the slope $\Delta f/\Delta p$ of the isotherm. Thus Ohm's law applies, $\tau = \sigma^{-1}\Delta f/\Delta p$. Here the mass current $\Delta f/\tau$ connected with filling or emptying is driven by the pressure difference Δp. The f dependence of the mass conductivity σ is displayed in Fig. 2. The results show that σ is roughly the same for adsorption and desorption and that there is little difference for the emptying of the D_s and the D_l segment. (Minimum values of σ are encountered, both for sample B and C, just before the completion of the D_s desorption, a fact that we cannot explain). Thus the emptying kinetics does not support the idea of pore blocking either. If there is any indication of such effects then it is the somewhat steeper slope of the D_l desorption step in sample B relative to sample C.

We conclude that even the pores of the present samples which are perhaps more regular and better controlled than many other examples of mesoporous substrates have to be regarded as a statistical ensemble of segments of varying diameter (or liquid-substrate interaction). Metastable states due to the quenched disorder [17] of this ensemble appear to be the most important aspect. It is not adequate to single out special local geometries such as the pore mouth, blind ends, or bottle necks. The idea of local pore blocking caused by an individual constriction of the pore should be abandoned for liquid (but not for solid) fillings of mesoporous networks. For the apparent asymmetry of adsorption and desorption we can cite no other reason than the broken particle-hole symmetry that is due to the liquid-matrix interaction in combination with random field type disorder. We think that the determination of pore space characteristics from adsorption/desorption isotherms is a problem still unsolved.

This work has been supported by the Deutsche Forschungsgemeinschaft (SFB 277).

[1] S. J. Gregg and K. S. W. Sing, *Adsorption, Surface Area, and Porosity* (Academic Press, New York, 1982).
[2] Y. C. Yortsos, *Methods in the Physics of Porous Media* (Academic Press, San Diego, 1999), Chap. 3, p. 69.
[3] L. D. Gelb *et al.*, Rep. Prog. Phys. **62**, 1573 (1999).
[4] V. Lehmann, R. Stengl, and A. Luigart, Mater. Sci. Eng. B **69**, 11 (2000).
[5] D. Kovalev *et al.*, Phys. Rev. Lett. **87**, 068301 (2001).
[6] B. Coasne *et al.*, Phys. Rev. Lett. **88**, 256102 (2002).
[7] J. C. Phillips, Rep. Prog. Phys. **59**, 1133 (1996).
[8] W. F. Saam and M. W. Cole, Phys. Rev. B **11**, 1086 (1975).
[9] L. Bruschi, A. Carlin, and G. Mistura, Phys. Rev. Lett. **89**, 166101 (2002).
[10] B. V. Derjaguin, Acta Physicochim. URSS **12**, 181 (1940).
[11] S. Dietrich, *Phase Transitions and Critical Phenomena* (Academic Press, London, 1988), Vol. 12, p. 1.
[12] B. V. Derjaguin and N. V. Churaev, J. Colloid Interface Sci. **54**, 157 (1976).
[13] J. C. P. Broekhoff and J. H. de Boer, J. Catal. **10**, 153 (1968).
[14] D. H. Everett and J. M. Haynes, J. Colloid Interface Sci. **38**, 125 (1972).
[15] K. G. Kornev, I. K. Shingareva, and A. V. Neimark, Adv. Colloid Interface Sci. **96**, 143 (2002).
[16] L. H. Cohan, J. Am. Chem. Soc. **60**, 433 (1938).
[17] E. Kierlik *et al.*, Phys. Rev. Lett. **87**, 055701 (2001).
[18] G. Mason, J. Colloid Interface Sci. **88**, 36 (1982); **95**, 277 (1983).
[19] M. Parlar and Y. C. Yortsos, J. Colloid Interface Sci. **124**, 162 (1988).
[20] P. C. Ball and R. Evans, Langmuir **5**, 714 (1989).
[21] V. P. Zhadanov, V. P. Fenelonov, and D. K. Efremov, J. Colloid Interface Sci. **120**, 218 (1987).
[22] M. Parlar and Y. C. Yortsos, J. Colloid Interface Sci. **132**, 425 (1989).
[23] P. I. Ravikovitch and A. V. Neimark, Langmuir **18**, 9830 (2002).
[24] L. Sarkisov and P. A. Monson, Langmuir **17**, 7600 (2001).
[25] V. Mayagoita, F. Rojas, and I. Kornhauser, J. Chem. Soc., Faraday Trans. 1 **81**, 2931 (1985).
[26] P. Huber and K. Knorr, Phys. Rev. B **60**, 12 657 (1999).